Journal of Medicinal Chemistry

ARTICLE

pubs.acs.org/jmc

Design and Synthesis of (+)-Discodermolide−Paclitaxel Hybrids Leading to Enhanced Biological Activity

Amos B. Smith, III,*[,†] Keizo Sugasawa,[†,§] Onur Atasoylu,[†] Chia-Ping Huang Yang,[‡] and Susan Band Horwitz*[,‡]

[†]Department of Chemistry, Monell Chemical Senses Center and Laboratory for Research on the Structure of Matter, University of Pennsylvania, Philadelphia, Pennsylvania 19104, United States

[‡]Department of Molecular Pharmacology, Albert Einstein College of Medicine, Bronx, New York 10461, United States

[§]Astellas Pharma Inc., Tsukuba-shi, Ibaraki 305-8585, Japan

Supporting Information

ABSTRACT:

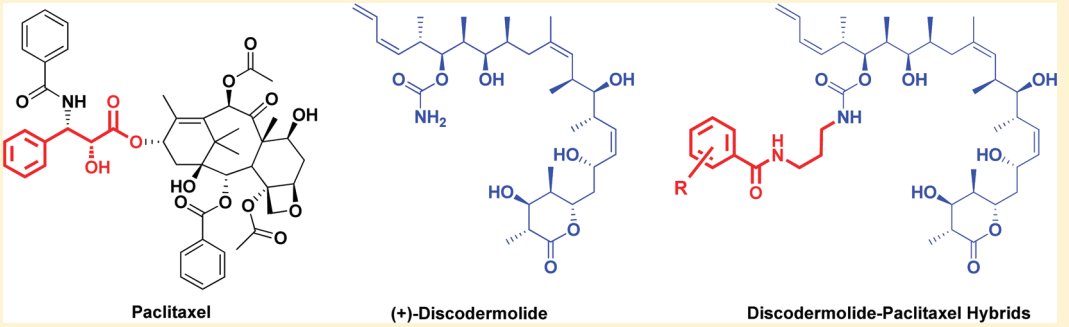

Potential binding modes of (+)-discodermolide at the paclitaxel binding site of tubulin have been identified by computational studies based on earlier structural and SAR data. Examination of the prospective binding modes reveal that the aromatic pocket occupied by the paclitaxel side chain is unoccupied by (+)-discodermolide. Based on these findings, a small library of (+)-discodermolide−paclitaxel hybrids have been designed and synthesized. Biological evaluation reveals a two- to eight-fold increase in antiproliferative activity compared to the parent molecule using the A549 and MCF-7 cancer cell lines.

INTRODUCTION

(+)-Discodermolide [(+)-**1**], a potent antitumor polyketide natural product, was first isolated in the early 1990s from extracts of the Caribbean marine sponge *Discodermia dissoluta* by Gunasekera and co-workers.[1] Confirmation of the assigned structure, as well as the absolute stereochemistry, was subsequently achieved by Schreiber and co-workers via total syntheses of the (−) enantiomer (1993), the natural (+) enantiomer (1994), and a number of novel analogues.[2,3] Initially reported to be a potent immunosuppressive agent, (+)-discodermolide was later recognized to possess significant antiproliferative activity both in vitro[4a] across the NCI panel of human cancer cell lines,[5] including paclitaxel resistant cell lines,[6] and in vivo.[4b] Like paclitaxel (**2**), (+)-discodermolide stabilizes tubulin thereby modulating microtubule dynamics that leads to cell arrest at mitosis (Figure 1).

As a result of the observed antitumor activity, (+)-discodermolide has generated significant interest in the synthetic community: 13 total syntheses have been reported to date.[7] Of particular significance, as recently recognized,[8] our four generation strategies exploited an early example of the Negishi coupling protocol to access the $C_{14}-C_{15}$ olefin.[7e,9] Subsequently, Novartis employed a similar cross-coupling tactic (i.e., Suzuki) to provide (+)-discodermolide for their phase I clinical trials.[10] Also early on, we also proposed[11] a solution conformation of (+)-discodermolide based on a combination of NMR data and the solid-state X-ray structure and carried out a comprehensive structure−activity relationship (SAR) study with Kosan Biosciences, Inc.[12,13]

More recently, we demonstrated that (+)-discodermolide both causes accelerated cell senescence[14] and binds to a region on β-tubulin close to the paclitaxel binding site.[15] Of interest here, (+)-discodermolide and paclitaxel act synergistically, not only in cell culture[16] but also in an ovarian xenograft tumor model in nude mice.[17] Subsequent studies, utilizing hydrogen/deuterium exchange and mass spectrometry, indicated that paclitaxel and discodermolide induce stability on opposite sides of the microtubule interface, suggesting a possible explanation for the synergy observed between these two drugs.[18] Finally, to

Received: May 31, 2011
Published: August 26, 2011

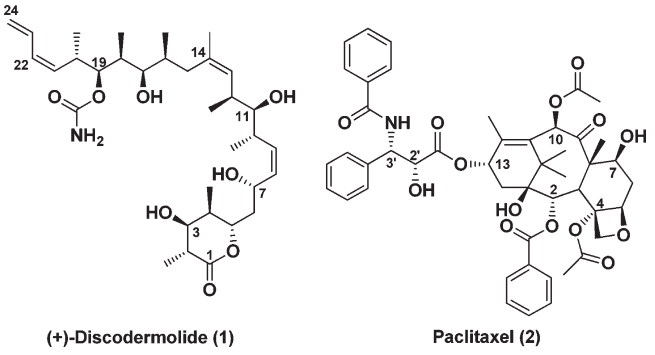

Figure 1. (+)-Discodermolide and paclitaxel.

decrease the pneumotoxicity of (+)-**1**, the presumptive cause leading to the failure of the Novartis phase I clinical trial,[10] possibly due to metabolites,[19] we extended our analogue program wherein the metabolically less stable lactone portion of the molecule[13a−c] and $C_{14}-C_{15}$ olefin[13d] were either individually or together replaced with isosteres. Pleasingly, these analogues preserved the cytotoxicity at a level similar to (+)-discodermolide (**1**).

However, despite the availability of extensive SAR data,[12] as well as structural,[1] computational and NMR studies,[11,20] the binding mode of (+)-discodermolide on tubulin remains unclear. Toward this end, we report here two possible binding modes of (+)-discodermolide in conjunction with the design, synthesis, and biological evaluation of (+)-discodermolide/paclitaxel hybrid molecules possessing photoaffinity labels.

In our SAR studies, we demonstrated the following: (1) that changes in the substitution pattern of C(1), C(3), and C(7) centers of (+)-discodermolide are favorable to retention of potent cytotoxicity, (2) that variations at the C(2), C(14), and the carbamate carbons are tolerable, and (3) that changes within the remaining portions of (+)-discodermolide significantly decrease the cytotoxicity.[12,13] On the basis of these observations, in conjunction with our earlier photoaffinity labeling study,[13e,f] we reasoned that the diene terminus of discodermolide resides in a hydrophobic/aromatic pocket, while the lactone moiety either occupies a binding pocket that can accommodate large groups or, more likely, is partially interfaced with the solvent. Further information gained from our earlier photoaffinity labeling study revealed that attachment of a large aromatic system (cf. benzophenone) and/or alkyl groups to the carbamate nitrogen did not significantly alter the observed activity.[13f] In fact, in two cases, comprising attachment of a *p*-dimethylaniline or *p*-benzophenone substituent at the carbamate nitrogen, a significant increase in tumor cell growth inhibitory activity was observed. We emphasize, however, that our earlier study was directed specifically at the preparation of photoaffinity labeled (+)-discodermolide analogues, with little or no attention focused on activity changes except for the possibility of increased hydrophobicity and/or conformational preferences. A closer examination of the earlier carbamate analogues, however, reveals a strong activity dependency both on the nature of the aromatic rings and linker length. On the basis of these observations, we have now examined the scope and molecular basis for the observed increase in cytotoxicity of these analogues exploiting detailed computational analysis.

The Solution Conformations of (+)-Discodermolide. In 2001, we reported that the preferred major solution conformation of (+)-discodermolide (**1**) was similar to the solid-state structure,[1] notwithstanding the 15 rotatable σ bonds.[11] In particular, variable temperature and cosolvent titration NMR studies provided evidence of intramolecular hydrogen bonds between the C(7)-OH and the C(1)-carbonyl, in conjunction with interactions between the carbamate nitrogen and the C(3) and C(7) hydroxyl groups. We postulated that *syn*-pentane interactions[21] were responsible for the proposed turn geometry of the backbone. Importantly, biological studies of epimers bearing inverted stereogenicities at the C(7), C(11), C(16), and C(17) revealed significantly lower activities, which led us to suggest that the conformation of the molecular segment between C(7)−C(17) is conserved upon binding. These conclusions were later confirmed by studies from other research laboratories.[20]

To understand more fully the solution behavior of (+)-discodermolide, we recently initiated computational studies exploiting molecular dynamics (MD) simulations. Monitoring backbone torsional angles over a 1 μs simulation period in water revealed the flexible torsional angles. It is of considerable interest that the lactone ring and the diene side chain moieties were found to display more flexibility compared to the rest of the molecule, when the turn geometry [i.e., C(7)−C(16)] was maintained throughout the simulation.

We next turned to NMR experiments to refine the solution conformation. The Distribution of Solution Conformations (DISCON) program developed in our laboratory[22] was employed to obtain a distribution of conformers based on NMR data. Earlier studies had revealed that (+)-discodermolide is more flexible in organic solvents.[20a,b] On the basis of this observation, acetonitrile was selected as the solvent for the NMR experiments, given that the aim of this study was to identify the "flexible" torsional angles and possible diverse conformational families for our pending docking studies. Proton−proton coupling constants and NOE derived distances reported earlier were utilized.[11] Deconvolution of the NMR observables over an ensemble of structures obtained by Monte Carlo conformational searches, followed by the clustering analysis that is embedded in the DISCON software, led to an ensemble of four principal conformers that in combination fit the NMR derived distance and torsional angle data better than any single conformation. Two conformers (Figure 2A,B), similar to the solid-state structure with differences in the lactone ring orientation, were identified as the major solution conformations (A, 35%; B, 32%), an observation fully consistent with our earlier solution structure.[11] Further examination of members of the major conformational families revealed (+)-discodermolide can adopt different conformations by adjusting the torsional angles around C(11)−C(12) and C(7) and C(8) bonds. In addition, the lactone ring can exist in equilibrium between chair, half-chair, and skew-boat conformations. The next most populated conformer (Figure 2C, 26%) comprised an inverted orientation at the diene region, wherein a different gauche orientation is preferred around the C(16)−C(17) and C(18)−C(19) bonds, with the remaining regions of (+)-discodermolide identical to the solid state structure. The remaining major family (Figure 2D, 7%) comprises both of these conformational changes and thereby forces the molecule to occupy an extended conformation. The distribution of the conformations can be rationalized by the observed $^3J_{H16-H17}$ and $^3J_{H11-H12}$ values of 6.2 and 6.6 Hz, respectively, corresponding to torsional angle averaging and by the observed NOE correlation variations from the solid-state structure, in particular those between H(7)−H(9), H(8)−H(12), H(9)−H(11), and H(12)−Me(18). Similar

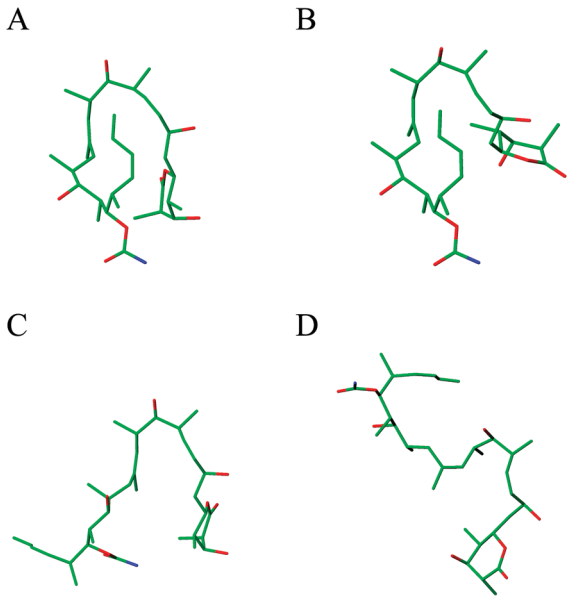

Figure 2. Solution conformations of (+)-discodermolide.

analyses reported earlier by the Jiménez-Barbero[20b] and the Snyder Laboratories[20c] are in accord with these observations, wherein differences in distributions were observed, presumably due to the differences in the solvents employed in the NMR experiments as well as to the force fields and clustering methods employed.

In summary, (+)-discodermolide in solution displays considerable flexibility in the orientation of the lactone and the diene/carbamate termini, with conservation of the turn region of the conformation comprising the C(7)−C(16) centers. For docking studies, we reasoned that the solution structures hold considerable importance because the bioactive conformation is more likely to exist in solution given that a lower energy penalty is paid for ligand reorganization upon binding (i.e., preorganization).[23] Stated differently, the 3D binding pharmacophore of the ligand is likely to be found in the conformation(s) that exist in solution, thus permitting easy recognition.[24]

Docking Studies. Having an understanding of the available major ensemble of solution conformations, we turned to define the binding mode of (+)-discodermolide on microtubules. In general, docking studies of microtubule stabilizing agents utilize the heterodimer α−β tubulin structure (PDB code: 1JFF) obtained by high resolution electron microscopy from the Zn induced crystalline sheets of tubulin in the presence of paclitaxel.[25] Although the tubulin structure in the crystal was shown to match the microtubule structure, it remains only an approximate model for docking studies for the following reasons: (1) the protein structure is distorted by the bound paclitaxel and thus does not necessarily represent the unbound microtubule,[26] (2) in vivo orientations and conformations of tubulin in microtubules and Zn-induced tubulin crystal sheets are different,[27] (3) the flexible M-loop region, at the taxane binding site is not well resolved,[25] (4) the lateral contacts between protofilaments, which are important for microtubule formation and tubulin dynamics[28] are missing, and (5) in humans the tubulin isotypes have different sequences than found in the reported protein structure.[29] Equally significant, the majority of reported (+)-discodermolide docking studies employ either the solid state conformation of (+)-discodermolide as a rigid scaffold or (+)-discodermolide is treated as a fully flexible molecule without regard to the accessible solution conformations.[15,18,30] Finally, earlier docking studies did not take into account the reported SAR data,[19] in particular the potent carbamate analogues.[13f]

More recently, Carlomagno[20a] and then Jiménez-Barbero et al.[20b] concluded, based on NMR transfer NOE studies of (+)-discodermolide and tubulin, that the binding conformation of (+)-discodermolide is identical to the solid state conformation with differences in the lactone ring portion and that (+)-discodermolide binds at the paclitaxel binding site. Paterson and co-workers in turn, based on these proposals, prepared a series of discodermolide−dictyostatin−paclitaxel hybrids which upon biological evaluation revealed a 20−35-fold *decrease* in tumor cell growth inhibition activity, employing the PANC-1 human cancer cell lines.[31] Notwithstanding these disappointing observations, we undertook docking studies employing the solution conformations identified by DISCON (vide infra).

Our 2009 hydrogen−deuterium exchange experiments also revealed that (+)-discodermolide binds to a region quite close to the paclitaxel site on β-tubulin, however, the stabilized microtubule geometries were different, as evidenced by the observed solvent exposure of the lateral sites,[18] with the most important interactions observed in the M-loop region of β-tubulin. On the basis of this information, we also chose to employ the paclitaxel site for docking studies. Beginning with the paclitaxel bound protein structure (PDB: 1JFF), paclitaxel was removed and the remaining protein structure was minimized with the OPLS-2005 force field to remove possible steric clashes. The binding site was not altered excessively, as we did not want to dock to a computationally generated binding pocket. Sets of (+)-discodermolide conformations, belonging to the families identified in solution (Figure 2A−D), were then docked, employing the Glide[32] and Molegro[33] software packages, treating the (+)-discodermolide conformations as rigid structures and the protein structure as flexible. Docking modes inconsistent with the SAR data were eliminated by visual inspection. We reason that this approach provides more valid criteria for finding a working binding hypothesis than calculated docking scores and energies due to the uncertainties (vide infra) in the protein structure (cf. Supporting Information for elimination criteria). Two binding poses for (+)-discodermolide were identified to be consistent with the SAR data.

The first pose (Figure 3B) orients the lactone end of (+)-discodermolide in a region occupied by the baccatin core of paclitaxel. The turn structure of (+)-discodermolide fits tightly in a region under the M-loop (β212−230), with the C(3) and C(7) hydroxyl groups forming hydrogen bonds to Pro272 and Thr274. In this pose, the carbamate moiety is directed toward the aromatic pocket that accommodates the paclitaxel tail (Figure 3A). The diene side chain and the lactone carbonyl group are directed toward the solvent, where additional substituents would appear to be tolerated. Rescoring of this pose via the MM/GBSA protocol[34] provided a favorable ΔG value of −12 kcal/mol. The second pose (Figure 3C), similar to pose 1, utilizes the (+)-discodermolide turn scaffold to fit in the hydrophobic pocket under the M-loop. This pose, however, orients the lactone moiety to the region where the paclitaxel C(2) benzoate group binds. This region would also appear to be able to accommodate larger groups while maintaining the activity of (+)-discodermolide analogues. That is, replacement of the lactone ring with other moieties might prove feasible. In this pose, the known decrease in activity of (+)-discodermolide analogues upon acetylation at the

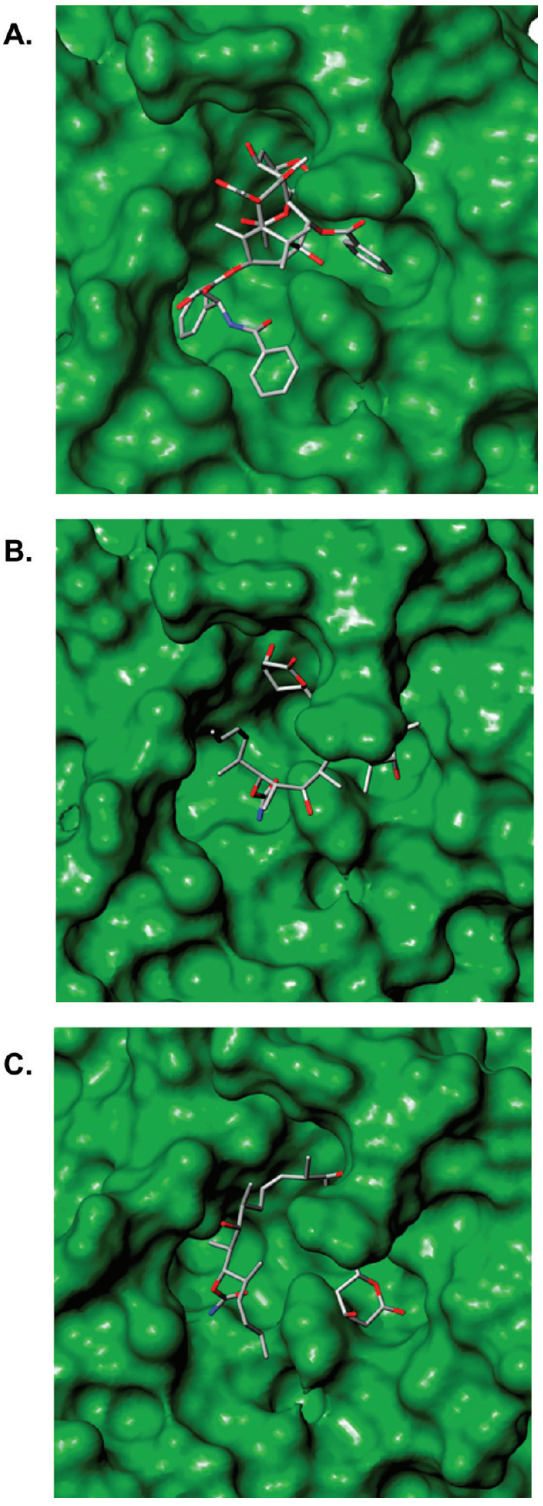

Figure 3. Binding mode of (A) paclitaxel (PDB: 1JFF), (B) (+)-discodermolide/pose 1, (C) (+)-discodermolide/pose 2.

C(11) hydroxyl group can be rationalized by the loss of a hydrogen bond to Thr274. This pose also orients the diene side chain in line with the paclitaxel benzamide group, with the (+)-discodermolide carbamate group directed to the C(3′)-phenyl pocket. Rescoring employing the MM/GBSA protocol again provided a favorable ΔG value of −18 kcal/mol. It is noteworthy that the Jiménez-binding mode differed significantly from the poses presented here and was found to be inconsistent with our SAR criteria.

Design of Hybrid Analogues. On the basis of the (+)-discodermolide docking modes, we designed a series of analogues that we reasoned would hold the promise of not only confirming our binding hypothesis, based initially on enhanced binding to tubulin and in turn enhanced cytotoxicity, but also define the true binding pose. Importantly, the design criteria were orchestrated to accommodate incorporation of photoaffinity labels for future structural studies.

Utilizing docking poses 1 and 2, we envisioned filling the aromatic pocket in the vicinity of the carbamate group, which in the case of paclitaxel is occupied by C(3′)-Ph group. In silico docking of our earlier carbamate analogues (vide infra), employing the identified (+)-discodermolide poses, revealed that the earlier analogues did not fully occupy the proposed pocket due to the shorter tether lengths. To test the validity of this scenario, analogues having aromatic groups attached to the carbamate group with differing tether lengths were generated (Figure 4).

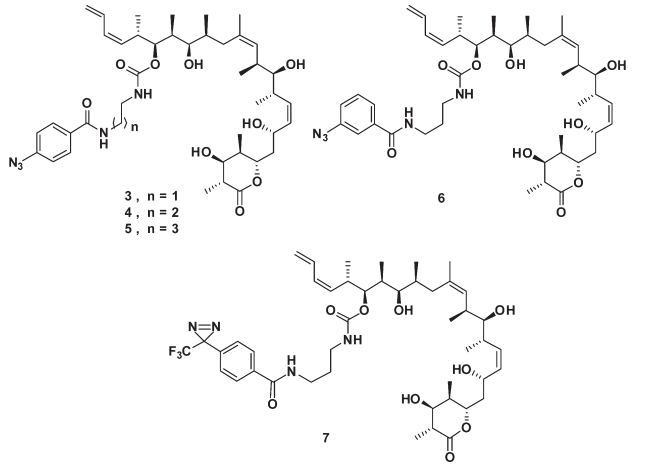

Figure 4. Designed (+)-discodermolide analogues.

We hypothesized that if the binding pocket is valid, the cytotoxic activities should vary, with the analogue possessing the most suitable linker length displaying the highest tumor cell growth inhibition activity. A second amide linkage was incorporated onto the tether to participate in a possible hydrogen bond, with Asp26 and His229 of β-tubulin, similar to the paclitaxel amide linkage. Finally, we envisioned that photoaffinity tags could be appropriately introduced without deleterious effects on the cytotoxicity. To this end, (+)-discodermolide/paclitaxel hybrid structures with a *p*-azidophenyl substituent (**3**−**5**, Figure 4) were generated. Docking studies were then conducted similar to the procedure applied for (+)-discodermolide. In these studies, the newly introduced paclitaxel C(3′)-phenyl group surrogates were permitted to be flexible, whereas the (+)-discodermolide core was kept rigid. Examination of the docking scores identified hybrid **4** to fill the aromatic pocket (Figure 5). Two additional hybrids **6** and **7** possessing different photoaffinity tags and optimal linker lengths were also designed to explore the potential effects of the hybrid structure motif as well as the photoaffinity groups on the cytotoxicity.

Synthesis of the Designed Analogues. The requisite hybrids, carrying the photoaffinity tags, were envisioned to arise via union of known (+)-discodermolide intermediate **19** (Scheme 1),[7e] prepared in connection with our gram-scale

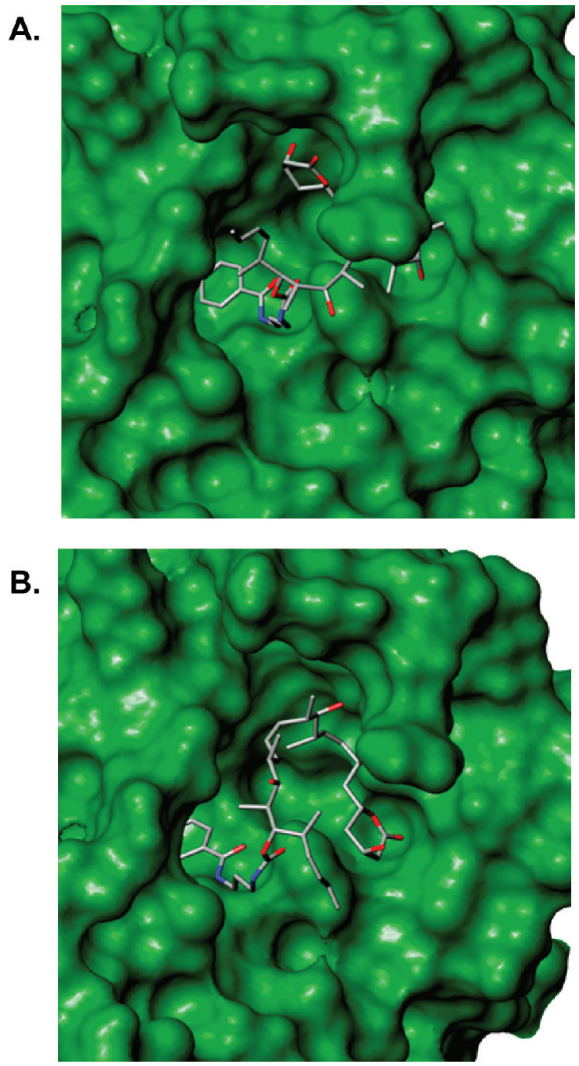

Figure 5. Docking of **4** in (A) pose 1 and (B) pose 2.

synthesis,[11] with the photoaffinity units bearing the suitable amine linkers. One of the attributes of developing preparative scale synthesis of architecturally complex natural products possessing significant bioregulatory properties is the subsequent ready availability of advanced intermediates for SAR and photoaffinity labeling studies.

To permit facile formation of carbamate linkage, the secondary alcohol on (+)-discodermolide would be activated as a carbonate ester (cf. **20**). The amine coupling partners were envisioned to arise via condensation reactions of the photoaffinity tags possessing carboxylic acid functionality with the diamine tethers of suitable length.

The photoaffinity tags for this study were prepared following known synthetic routes,[35−37] wherein acids **8** and **13** were activated as hydroxysuccinamide esters,[38] followed by condensation with the alkyl diamine linkers (Scheme 2). For the aryl-(trifluoromethyl)diazirine component **18**, the mono-Boc protected amine linker was employed with *N*,*N*′-carbonyl-diimidazole (CDI)[39] to reduce possible side reactions; the Boc group was subsequently removed under acidic conditions.

In the event, construction of (+)-discodermolide/paclitaxel hybrids **3**−**7** (Scheme 3), possessing the phototags, entailed a

Scheme 1. Retrosynthetic Analysis of Hybrid Molecules

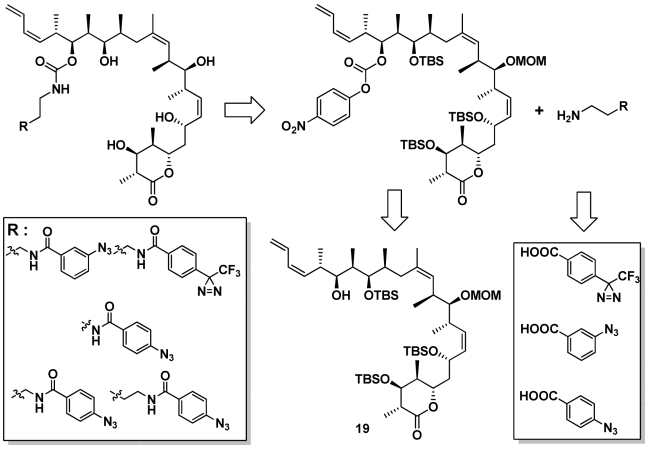

Scheme 2. Preparation of the Photoaffinity Tags

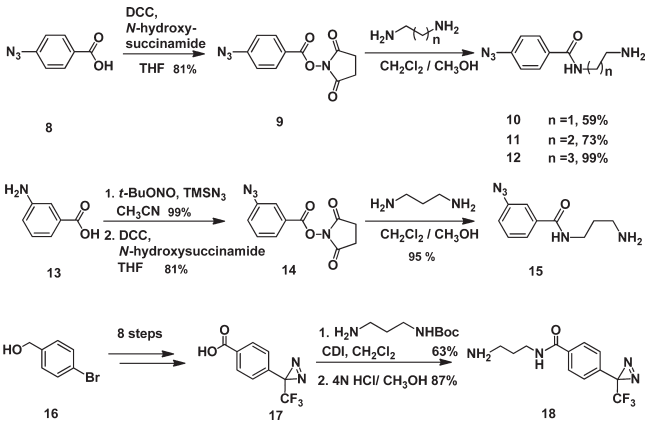

Scheme 3. Syntheses of the Designed Analogues

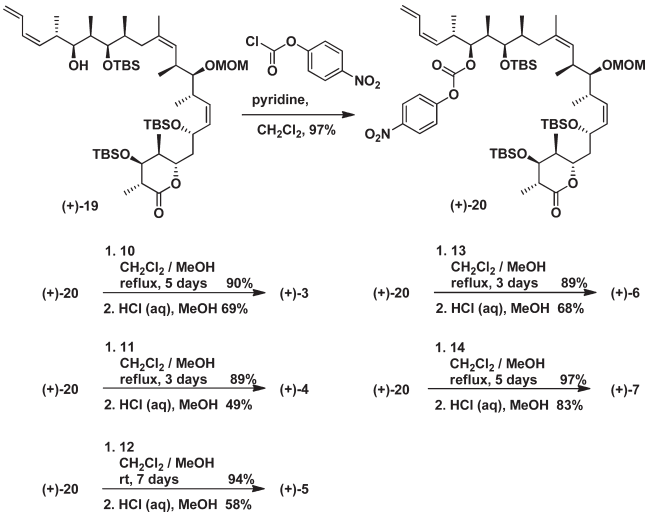

two-step protocol wherein the secondary alcohol in (+)-**19** was converted to a *p*-nitrophenylcarbonate ester, followed by union

dx.doi.org/10.1021/jm200692n |*J. Med. Chem.* 2011, 54, 6319–6327

Table 1. Cytotoxicity of (+)-Discodermolide and Analogues against Human Lung A549 and Breast MCF-7 Cancer Cell Lines

IC_{50}[a]	(+)-**1**	(+)-**2**	(+)-**3**	(+)-**4**	(+)-**5**	(+)-**6**	(+)-**7**
A549	9.34 ± 0.56	3.14 ± 0.09	5.61 ± 0.15	1.21 ± 0.35	3.76 ± 0.57	1.05 ± 0.15	2.64 ± 0.22
MCF-7	7.98 ± 0.35	0.91 ± 0.11	3.64 ± 0.12	1.90 ± 0.43	2.71 ± 0.55	1.66 ± 0.48	1.92 ± 0.07

[a] IC_{50} equals the concentration (nM) of drug that inhibits 50% cell growth.

with amines **10**−**12** and **15** and **18**.[40] Global deprotection under acidic conditions provided (+)-**3**−(+)-**7** in good to excellent yields. Importantly, the synthetic route not only provides facile access to the designed (+)-discodermolide/paclitaxel hybrids possessing the photoaffinity tags, but was also designed to permit ready access to either ^{3}H or ^{14}C analogues for future labeling experiments (Scheme 3).

Biological Evaluations of the (+)-Discodermolide/Paclitaxel Hybrids. The designed (+)-discodermolide/paclitaxel hybrids possessing the photoaffinity labels were tested for antiproliferative activity against human lung (A549) and breast (MCF-7) cancer cell lines. Discodermolide [(+)−1] and paclitaxel (2) served as controls. In accord with our design strategy, the analogues revealed improved activity in a trend changing with the tether length (Table 1).

Given the similarity of the analogues, the up to an 8-fold increase in potency is believed to be associated with an interaction with the proposed aromatic pocket and not simply to an increase in hydrophobicity or other factors. Also of importance, (+)-discodermolide and each of the six analogues increased the amount of microtubule polymerization compared to the control that had no drug added (Figure 6). Taken together, these observations strongly suggest that all of the discodermolide molecules have the same mechanism of action.

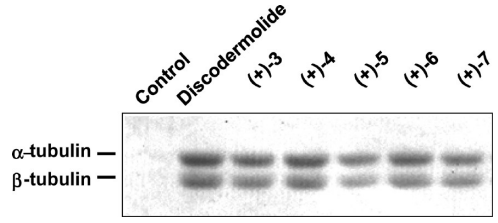

Figure 6. Tubulin polymerization in the presence of (+)-discodermolide and its analogues. The control has no drug.

In summary, we have defined two possible binding modes for (+)-discodermolide in the paclitaxel binding pocket. To test the validity of the proposed modes, we designed and synthesized a series of hybrid molecules wherein the aromatic ring of paclitaxel was attached to (+)-discodermolide, exploiting a tether of suitable length. Biological testing demonstrated that hybrid congeners possess increased potency compared to (+)-discodermolide. Given the availability of the already incorporated phototags, the discodermolide/paclitaxel hybrids hold the promise of defining the (+)-discodermolide binding site and mode of action, as well as determining whether the drug demonstrates selectivity for any of the 7 β-tubulin isotypes. Because certain isotypes, particularly βIII-tubulin, have been associated with paclitaxel resistance,[41] an investigation of the interaction between drugs and specific tubulin isotypes becomes an important goal, and in particular definition of human tubulin isotypes that bind (+)-discodermolide. Such studies in conjunction with radiolabeling experiments are ongoing in our laboratories.

EXPERIMENTAL SECTION

Experimental Details for Obtaining IC_{50} Values. Cells lines were obtained from the American Type Culture Collection (ATCC) and maintained in RPMI medium supplemental with 10% fetal bovine serum. Cells (800 A549 or 2000 MCF-7) were added to each well of a 96-well plate. Increasing concentrations of the indicated drugs were added 18 h after plating. IC_{50} values, the concentration of drug that inhibits cell growth by 50%, were determined after 72 or 96 h incubation at 37 °C for A549 or MCF-7 cells, respectively, using the SRB method.[40] The two cell lines were fixed and stained at different times to take into account their different growth rates.

Experimental Details for Tubulin Polymerization Studies. Bovine brain tubulin (2.5 μM) from Cytoskeleton Inc. in a buffer containing 0.1 M MES, 1 mM EGTA, and 1 mM $MgCl_2$ was incubated with 3 μM of the indicated drugs, in the presence of 2 mM GTP, at 37 °C for 30 min. Samples were centrifuged at 120000*g* at 37 °C for 1 h, and the pellet that contains the polymerized tubulin was dissolved in SDS sample buffer and analyzed by SDS-polyacrylamide gel electrophoresis. Proteins were then transferred to nitrocellulose and stained with *Ponceau S*.

Experimental Details for Synthesis and Characterization. Except as otherwise indicated, all reactions were run under an argon atmosphere in flame- or oven-dried glassware, and solvents were freshly distilled. The argon was deoxygenated and dried by passage through an OXICLEAR filter from Aldrich and Drierite tube, respectively. Diethyl ether (Et_2O), tetrahydrofuran (THF), and dichloromethane (CH_2Cl_2) were purchased from Aldrich (HPLC purity) and further purified by Pure Solve PS-400. All other reagents were purchased from Aldrich or Acros and used as received. Reactions were monitored by thin layer chromatography (TLC) either with 0.25 mm of Silicycle or 0.25 mm of E. Merck (Kieselgel $60F_{254}$, Merck) precoated silica gel plates. Silica gel for flash chromatography (particle size 0.040−0.063 mm) was supplied by Silicycle or Sorbent. Yields refer to chromatographically and spectroscopically pure compounds unless otherwise noted. ^{1}H and ^{13}C spectra were recorded on a Bruker AMX-500 spectrometer. Chemical shifts are reported as δ values relative to internal chloroform (δ 7.26) or benzene (δ 7.15) for ^{1}H and either chloroform (δ 77.0) or benzene (δ 128.0) for ^{13}C. Infrared spectra were recorded on a Jasco FTIR-480plus spectrometer. Optical rotations were measured on a Jasco P-2000 polarimeter in the solvent indicated. High resolution mass spectra were measured at the University of Pennsylvania Mass Spectrometry Center on either a VG Micromass 70/70H or VG ZAB-E spectrometer. Analytical reverse-phased (Sunfire C18; 4.6 mm × 50 mm, 5 mL) high-performance liquid chromatography (HPLC) was performed with a Waters binary gradient module 2525 equipped with Waters 2996 PDA and Waters micromass ZQ. All final compounds were analyzed employing a linear gradient from 10% to 90% of acetonitrile in water over 8 min and a flow rate of 1 mL/min and, unless otherwise stated, the purity level was >95%.

Representative Synthetic Procedures. *Synthesis of (+)-**3a**.* Compound (+)-**20** (80 mg, 0.0725 mmol) was dissolved in CH_2Cl_2 (1 mL) and MeOH (1 mL). *N*-(4-Azido-benzoyl)-1,2-ethanediamine (**10**) (45 mg, 0.218 mmol) in MeOH (1 mL) and Et_3N (40 μL, 0.290 mmol) were added to the above solution. The resultant solution was stirred at room temperature for 6 days. Water (50 mL) was added to the reaction mixture and extracted with CH_2Cl_2 (3 × 50 mL). The combined organic layers were washed with brine (50 mL), dried over

$MgSO_4$, filtered, and concentrated. Flash chromatography (11−25% EtOAc in hexane) provided compound (+)-**3a** (75.1 mg, 89% yield) as a colorless amorphous solid. $[\alpha]^{22}_D$ = +36.0° (*c* = 0.65, $CHCl_3$). IR (film, NaCl): 3336, 2957, 2929, 2857, 2123, 1718, 1653, 1604, 1539, 1500, 1254, 1044, 836, 775 cm^{-1}. ^1H NMR (500 MHz, $CDCl_3$) δ: 7.81 (d, *J* = 8.3 Hz, 2H), 7.33 (brs, 1H), 7.03 (d, *J* = 8.4 Hz, 2H), 6.54 (ddd, *J* = 16.7, 10.6, 10.6 Hz, 1H), 5.88 (apparent t, *J* = 10.9 Hz, 1H), 5.35−5.13 (m, 5H), 5.11 (d, *J* = 10.2 Hz, 1H), 5.02 (d, *J* = 9.9 Hz, 1H), 4.81 (apparent t, *J* = 9.1 Hz, 1H), 4.74 (apparent t, *J* = 5.8 Hz, 1H), 4.59 (ABq, J_{AB} = 6.9 Hz, Δ_{AB} = 28.4 Hz, 2H), 4.50 (apparent t, *J* = 10.3 Hz, 1H), 3.63 (brs, 1H), 3.56−3.44 (m, 3H), 3.41 (apparent t, *J* = 4.0 Hz, 1H), 3.39−3.30 (m, 1H), 3.34 (s, 3H), 3.06 (apparent t, *J* = 5.6 Hz, 1H), 2.99−2.91 (m, 1H), 2.75−2.66 (m, 1H), 2.60 (qd, *J* = 7.5, 2.8 Hz, 1H), 2.55−2.47 (m, 1H), 2.06 (apparent t, *J* = 12.7 Hz, 1H), 1.91−1.76 (m, 3H), 1.75−1.66 (m, 2H), 1.63−1.54 (m, 1H), 1.57 (s, 3H), 1.23 (d, *J* = 7.6 Hz, 3H), 0.96 (d, *J* = 6.7 Hz, 3H), 0.95−0.84 (m, 12H), 0.91 (s, 9H), 0.87 (s, 9H), 0.85 (s, 9H), 0.72 (d, *J* = 6.7 Hz, 3H), 0.08 (s, 3H), 0.06 (s, 3H), 0.054 (s, 3H), 0.048 (s, 3H), 0.04 (s, 3H), 0.03 (s, 3H). ^{13}C NMR (125 MHz, $CDCl_3$) δ: 173.6, 166.7, 158.8, 143.4, 133.9, 133.4, 132.3, 132.1, 132.0, 131.1, 130.8, 130.0, 129.0, 119.1, 118.5, 97.5, 86.4, 79.5, 77.3, 77.0, 74.9, 64.9, 56.2, 44.2, 42.7, 42.5, 40.5, 37.9, 36.1, 35.8, 35.7, 34.6, 34.4, 34.3, 26.4, 26.1, 25.9, 23.3, 18.7, 18.3, 18.1, 17.7, 16.8, 16.7, 16.5, 14.4, 14.2, 10.2, −3.2, −3.5, −4.2, −4.3, −4.66, −4.68. High resolution mass spectrum (ESI+) *m*/*z* 1190.7408 ($(M + Na)^+$; calcd for $C_{62}H_{109}N_5O_{10}Si_3Na$: 1190.7380).

*Synthesis of (+)-**3***. To a solution of compound (+)-**3a** (67 mg, 0.0573 mmol) in MeOH (5 mL) was added aqueous hydrochloric acid (4M, 4 mL) in 100−250 μL portions over 7 h at a rate which minimized precipitation (ca. 8−30 min intervals), and the sides of flask were rinsed with MeOH (1 mL). The reaction mixture was stirred at room temperature for 18 h and diluted with EtOAc (70 mL). The resulting solution was neutralized with $NaHCO_3$ (1.35 g in H_2O 18 mL) at 0 °C. Phosphate buffer pH 7 (1M, 30 mL) and NaCl (17 g) were added, and the aqueous layer was extracted with EtOAc (3 × 70 mL). The combined organic layers were washed with brine (100 mL), dried over $MgSO_4$, filtered, and concentrated. The residue was purified three times by flash chromatography (80% EtOAc in hexane or 3−6% MeOH/CH_2Cl_2) to afford compound (+)-**3** (31.1 mg, 69% yield) as a colorless amorphous solid. $[\alpha]^{22}_D$ = +17.4° (*c* = 0.10, $CHCl_3$). IR (film, NaCl): 3359, 2968, 2123, 1699, 1639, 1604, 1543, 1501, 1457, 1284, 1120, 1032, 731 cm^{-1}. ^1H NMR (500 MHz, $CDCl_3$) δ: 7.81 (d, *J* = 8.5 Hz, 2H), 7.26 (br, 1H), 7.06 (d, *J* = 8.4 Hz, 2H), 6.55 (ddd, *J* = 16.6, 10.6, 10.6 Hz, 1H), 5.84 (apparent t, *J* = 11.0 Hz, 1H), 5.54−5.41 (m, 3H), 5.26 (t, *J* = 10.4 Hz, 1H), 5.17−5.05 (m, 3H), 4.76−4.66 (m, 2H), 4.61 (apparent t, *J* = 9.3 Hz, 1H), 3.70 (br m, 1H), 3.57−3.44 (m, 2H), 3.43−3.31 (m, 2H), 3.29−3.16 (m, 3H), 3.00−2.91 (m, 1H), 2.83−2.74 (m, 1H), 2.68 (qd, *J* = 7.3, 4.6 Hz, 1H), 2.63−2.51 (m, 2H), 2.40−2.20 (br, 2H), 2.00−1.74 (m, 6H), 1.69−1.62 (m, 1H), 1.58 (s, 3H), 1.28 (d, *J* = 7.3 Hz, 3H), 1.06 (d, *J* = 6.9 Hz, 3H), 1.01 (d, *J* = 6.8 Hz, 3H), 0.93 (apparent d, *J* = 6.8 Hz, 6H), 0.90 (d, *J* = 6.6 Hz, 3H), 0.82 (d, *J* = 6.5 Hz, 3H). ^{13}C NMR (125 MHz, $CDCl_3$) δ: 174.6, 167.2, 158.4, 143.6, 134.5, 133.9, 133.6, 133.0, 132.3, 130.6, 130.0, 129.6, 129.1, 119.2, 118.3, 79.4, 78.9, 77.4, 75.2, 73.1, 64.4, 43.3, 42.0, 41.2, 40.5, 37.4, 36.2, 36.0, 35.94, 35.91, 34.9, 33.0, 23.4, 18.8, 17.5, 16.7, 15.7, 14.2, 12.8, 9.3. High resolution mass spectrum (ESI+) *m*/*z* 804.4495 ($(M + Na)^+$; calcd for $C_{42}H_{63}N_5O_9Na$: 804.4523).

■ ASSOCIATED CONTENT

Supporting Information. ^1H and ^{13}C NMR spectra, experimental methods and synthetic procedures of (+)-**3**−(+)-**20**; HPLC data of (+)-**3**−(+)-**7** used in biological assays; NMR data utilized in solution conformation calculations; SAR data employed in computational studies. This material is available free of charge via the Internet at http://pubs.acs.org.

■ AUTHOR INFORMATION

Corresponding Author

*For A.B.S.: phone, (215) 898-4860; fax, (215) 898-5129; E-mail, smithab@sas.upenn.edu. For S.B.H.: phone, (718) 430-2163; fax, (718) 430-8922; E-mail, susan.horwitz@einstein.yu.edu.

■ ACKNOWLEDGMENT

Support was provided by the National Institutes of Health through the National Institutes of General Medical Sciences and the National Cancer Institute through grants GM-29028 (A.B.S.) and CA-077263 (S.B.H.), and the Breast Cancer Research Foundation (S.B.H.). We also thank Drs. G. Furst and R. Kohli of the Department of Chemistry NMR and MS Facilities for obtaining the NMR and high resolution mass spectra.

■ ABBREVIATIONS USED

ESI-HMRS, electrospray ionization high-resolution mass spectrometry; TMS, tetramethylsilane; TLC, thin layer chromatography; PDB, Protein Data Bank; DISCON: distribution of solution conformationsNCI, National Cancer Institute; SAR, structure−activity relationship; MD, molecular dynamics; CDI, *N*,*N*′-carbonyl-diimidazole

■ REFERENCES

(1) (a) Gunasekera, S. P.; Gunasekera, M.; Longley, R. E.; Shulte, K. Discodermolide: a new bioactive polyhydroxylated lactone from the marine sponge *Discodermia dissolute*. *J. Org. Chem.* **1990**, *55*, 4912–4912. (b) Additions and corrections. *J. Org. Chem.* **1991**, *56*, 1346.

(2) Nerenberg, J. B.; Hung, D. T.; Somers, P. K.; Schreiber, S. L. Total synthesis of the immunosup-pressive agent (−)-discodermolide. *J. Am. Chem. Soc.* **1993**, *115*, 12621–12622.

(3) Hung, D. T.; Nerenberg, J. B.; Schreiber, S. L. Distinct binding and cellular properties of synthetic (+)- and (−)-discodermolides. *Chem. Biol.* **1994**, *1*, 67–71.

(4) (a) Longley, R. E.; Caddigan, D.; Harmody, D.; Gunasekera, M.; Gunasekera, S. P. Discodermolide—A new, marine-derived immunosuppressive compound. I. In vitro studies. *Transplantation* **1991**, *52*, 650–656. (b) Longley, R. E.; Caddigan, D.; Harmody, D.; Gunasekera, M.; Gunasekera, S. P. Discodermolide—A new, marine-derived immunosuppressive compound. II. In vivo studies. *Transplantation* **1991**, *52*, 656–661.

(5) Data is available through Development Therapeutics Program website from NIH: http://dtp.nci.nih.gov

(6) Kowalski, R. J.; Giannakakou, P.; Gunasekera, S. P.; Longley, R. E.; Day, B. W.; Hamel, E. The microtubule-stabilizing agent discodermolide competitively inhibits the binding of paclitaxel (taxol) to tubulin polymers, enhances tubulin nucleation reactions more potently than paclitaxel, and inhibits the growth of paclitaxel-resistant cells. *Mol. Pharmacol.* **1997**, *52*, 613–622.

(7) (a) See ref 2. (b) Smith, A. B., III; Qiu, Y.; Jones, D. R.; Kobayashi, K. Total synthesis of (−)-discodermolide. *J. Am. Chem. Soc.* **1995**, *117*, 12011–12012. (c) Harried, S. S.; Yang, G.; Strawn, M. A.; Myles, D. C. Total Synthesis of (−)-Discodermolide: An Application of a Chelation-Controlled Alkylation Reaction. *J. Org. Chem.* **1997**, *62*, 6098–6099. (d) Marshall, J. A.; Johns, B. A. Total Synthesis of (+)-Discodermolide. *J. Org. Chem.* **1998**, *63*, 7885–7892. (e) Smith, A. B., III; Kaufman, M. D.; Beauchamp, T. J.; LaMarche, M. J.; Arimoto, H. Gram Scale Synthesis of (+)-Discodermolide. *Org. Lett.* **1999**, *1*, 1823–1826. (f) Paterson, I.; Florence, G. J.; Gerlach, K.; Scott, J. P.;

Sereing, N. A practical synthesis of (+)-discodermolide and analogues: Fragment union by complex aldol reactions. *J. Am. Chem. Soc.* **2001**, *123*, 9535–9544. (g) Smith, A. B., III; Freeze, S. B.; Brouard, I.; Hirose, T. A Practical Improvement, Enhancing the Large-Scale Synthesis of (+)-Discodermolide: A Third-Generation Approach. *Org. Lett.* **2003**, *5*, 4405–4408. (h) Paterson, I.; Delgado, O.; Florence, G. J.; Lyothier, I.; Scott, J. P.; Sereinig, N. 1,6-Asymmetric induction in boron-mediated aldol reactions: Application to a practical total synthesis of (+)-discodermolide. *Org. Lett.* **2003**, *5*, 35–38. (i) Mickel, S. J.; Sedelmeier, G. H.; Niederer, D.; Daeffler, R.; Osmani, A.; Schreiner, K.; Seeger-Weibel, M.; Berod, B.; Schaer, K.; Gamboni, R.; Chen, S.; Chen, W.; Jagoe, C. T.; Kinder, F. R.; Loo, M.; Prasad, K.; Shieh, W. C.; Wang, R. M.; Waykole, L.; Xu, D. D.; Xue, S. Large-Scale Synthesis of the Anticancer Marine Natural Product (+)-Discodermolide. Part 5: Linkage of Fragments C(1)-(6) and C(7)-(24) and Finale. *Org. Process Res. Dev.* **2004**, *8*, 122–130. (j) Paterson, I.; Lyothier, I. Total synthesis of (+)-discodermolide: An improved endgame exploiting a Still–Gennari-type olefination with a C1-C8 β-ketophosphonate fragment. *Org. Lett.* **2004**, *6*, 4933–4936. (k) Arefolov, A.; Panek, J. Crotylsilane reagents in the synthesis of complex polyketide natural products: Total synthesis of (+)-discodermolide. *J. Am. Chem. Soc.* **2005**, *127*, 5596–5603. (l) Smith, A. B., III; Freeze, B. S.; Xian, M.; Hirose, T. Total synthesis of (+)-discodermolide: A highly convergent fourth-generation approach. *Org. Lett.* **2005**, *7*, 1825–1828. (m) Lemos, E.; Porée, F.-H.; Bourin, A.; Barbion, J.; Agouridas, E.; Lannou, M.-I.; Commerçon, A.; Betzer, J.-F.; Pancrazi, A.; Ardisson, J. Total synthesis of discodermolide: Optimization of the effective synthetic route. *Chem.—Eur. J.* **2008**, *14*, 11092–11112.

(8) Fernholm, A. In *A Powerful Tool for Chemists*; Nobel Prize 2010, Information for Public; Bäckvall, J.-E. Thelander, L., Eds.; The Royal Swedish Academy of Sciences, 2010; http://nobelprize.org/nobel_prizes/chemistry/laureates/2010/info_publ_eng_2010.pdf

(9) Beauchamp, T. J.; LaMarche, M. J.; Kaufman, M. D.; Qiu, Y. P.; Arimoto, H.; Jones, D. R.; Kobayashi, K. Evolution of a Gram-Scale Synthesis of (+)-Discodermolide. *J. Am. Chem. Soc.* **2000**, *122*, 8654–8664.

(10) Mita, A.; Lockhart, A. C.; Chen, T. L.; Bochinski, K.; Curtright, J.; Cooper, W.; Hammond, L.; Rothenberg, M.; Rowinsky, E.; Sharma, S. A phase I pharmacokinetic (PK) trial of XAA296A (Discodermolide) administered every 3 wks to adult patients with advanced solid malignancies. *J. Clin. Oncol. ASCO Annu. Meet. Proc.* **2004**, *14S*, 2025.

(11) Smith, A. B., III; LaMarche, M. J.; Falcone-Hindley, M. Solution Structure of (+)-Discodermolide. *Org. Lett.* **2001**, *3*, 695–698.

(12) See review article and reference therein:Smith, A. B., III; Freeze, B. S. (+)-Discodermolide: total synthesis, construction of novel analogues, and biological evaluation. *Tetrahedron* **2008**, *64*, 261–298.

(13) (a) Burlingame, M. A.; Shaw, S. J.; Sundermann, K. F.; Zhang, D.; Petryka, J.; Mendoza, E.; Liu, F.; Myles, D. C.; LaMarche, M. J.; Hirose, T.; Freeze, B. S.; Smith, A. B., III A series of 23,24-dihydrodiscodermolide analogues with simplified lactone regions. *Bioorg. Med. Chem. Lett.* **2004**, *14*, 2335–2338. (b) Shaw, S. J.; Sundermann, K. F.; Burlingame, M. A.; Myles, D. C.; Freeze, B. S.; Xian, M.; Brouard, I.; Smith, A. B., III Toward understanding how the lactone moiety of discodermolide affects activity. *J. Am. Chem. Soc.* **2005**, *127*, 6532–6533. (c) Shaw, S. J.; Menzella, H. G.; Myles, D. C.; Xian, M.; Smith, A. B. Coumarin-derived discodermolide analogues possessing equivalent antiproliferative activity to the natural product—A further simplification of the lactone region. *Org. Biomol. Chem.* **2007**, *5*, 2753–2755. (d) Smith, A. B.; Freeze, S. B.; LaMarche, M. J.; Hirose, T.; Brouard, I.; Xian, M.; Sundermann, K. F.; Shaw, S. J.; Burlingame, M. A.; Horwitz, S. B.; Myles, D. C. Design, Synthesis, and Evaluation of Analogues of (+)-14-Normethyldiscodermolide. *Org. Lett.* **2005**, *7*, 315–318. (e) Smith, A. B.; Freeze, B. S.; LaMarche, M. J.; Hirose, T.; Brouard, I.; Rucker, P. V.; Xian, M.; Sundermann, K. F.; Shaw, S. J.; Burlingame, M. A.; Horwitz, S. B.; Myles, D. C. Design, synthesis, and evaluation of carbamate-substituted analogues of (+)-discodermolide. *Org. Lett.* **2005**, *7*, 311–314. (f) Smith, A. B.; Rucker, P. V.; Brouard, I.; Freeze, B. S.; Xia, S. J.; Horwitz, S. B. Design, synthesis, and biological evaluation of potent discodermolide fluorescent and photoaffinity molecular probes. *Org. Lett.* **2005**, *7*, 5199–5202.

(14) Klein, L. E.; Freeze, B. S.; Smith, A. B.; Horwitz, S. B., III The microtubule stabilizing agent discodermolide is a potent inducer of accelerated cell senescence. *Cell Cycle* **2005**, *4*, 501–507.

(15) Xia, S.; Kenesky, C. S.; Rucker, P. V.; Smith, A. B., III; Orr, G. A.; Horwitz, S. B. A photoaffinity analogue of discodermolide specifically labels a peptide in β-tubulin. *Biochemistry* **2006**, *45*, 11762–11775.

(16) (a) Martello, L. A.; McDaid, H. M.; Regl, D. L.; Yang, C. P. H.; Meng, D. F.; Pettus, T. R. R.; Kaufman, M. D.; Arimoto, H.; Danishefsky, S. J.; Smith, A. B.; Horwitz, S. B. Taxol and discodermolide represent a synergistic drug combination in human carcinoma cell lines. *Clin. Cancer Res.* **2000**, *6*, 1978–1987. (b) Honore, S.; Kamath, K.; Braguer, D.; Horwitz, S. B.; Wilson, L.; Briand, C.; Jordan, M. A. Synergistic suppression of microtubule dynamics by discodermolide and paclitaxel in non-small cell lung carcinoma cells. *Cancer Res.* **2004**, *64*, 4957–4964.

(17) Huang, G. S.; Lopez-Barcons, L.; Freeze, B. S.; Smith, A. B., III; Goldberg, G. L.; Horwitz, S. B.; McDaid, H. M. Potentiation of taxol efficacy and by discodermolide in ovarian carcinoma xenograft-bearing mice. *Clin. Cancer Res.* **2006**, *12*, 298–304.

(18) Khrapunovich-Baine, M.; Menon, V.; Verdier-Pinard, P.; Smith, A. B.; Angeletti, R. H.; Fiser, A.; Horwitz, S. B.; Xiao, H. Distinct Pose of Discodermolide in Taxol Binding Pocket Drives a Complementary Mode of Microtubule Stabilization. *Biochemistry* **2009**, *48*, 11664–11677.

(19) Fan, Y.; Schreiber, E. M.; Day, B. W. Human Liver Microsomal Metabolism of (+)-Discodermolide. *J. Nat. Prod.* **2009**, *72*, 1748–1754.

(20) (a) Sanchez-Pedregal, V. M.; Kubicek, K.; Meiler, J.; Lyothier, I.; Paterson, I.; Carlomagno, T. The tubulin-bound conformation of discodermolide derived by NMR studies in solution supports a common pharmacophore model for epothilone and discodermolide. *Angew. Chem.* **2006**, *45*, 7388–7394. (b) Canales, A.; Matesanz, R.; Gardner, N. M.; Andreu, J. M.; Paterson, I.; Diaz, J. F.; Jimenez-Barbero, J. The bound conformation of microtubule-stabilizing agents: NMR insights into the bioactive 3D structure of discodermolide and dictyostatin. *Chem.—Eur. J.* **2008**, *14*, 7557–7569. (c) Jogalekar, A. S.; Kriel, F. H.; Shi, Q.; Cornett, B.; Cicero, D.; Snyder, J. P. The Discodermolide Hairpin Structure Flows from Conformationally Stable Modular Motifs. *J. Med. Chem.* **2010**, *53*, 155–165.

(21) Hoffmann, R. W.; Stenkamp, D.; Trieselmann, T.; Göttlich, R. Flexible molecules with defined shape. XI. Conformer equilibria in 2,4-disubstituted pentane derivatives. *Eur. J. Org. Chem.* **1999**, *11*, 2915–2927.

(22) Information of DISCON software will be provided in a subsequent report; also see http://discon.sourceforge.net/.

(23) (a) Cram, D. J. Preorganization—From Solvents to Spherands. *Angew. Chem., Int. Ed. Engl.* **1986**, *25*, 1039–1057. (b) Houk, K. N.; Leach, A. G.; Kim, S. P.; Zhang, X. Binding Affinities of Host–Guest, Protein–Ligand, and Protein–Transition-State Complexes. *Angew. Chem., Int. Ed.* **2003**, *42*, 4872–4897.

(24) (a) Perola, E.; Charifson, P. S. Conformational Analysis of Drug-Like Molecules Bound to Proteins: An Extensive Study of Ligand Reorganization upon Binding. *J. Med. Chem.* **2004**, *47*, 2499–2510. (b) Butler, K. T.; Luque, F. J.; Barril, X. Toward Accurate Relative Energy Predictions of the Bioactive Conformation of Drugs. *J. Comput. Chem.* **2009**, *30*, 601–610.

(25) Lowe, J.; Li, H.; Downing, K. H.; Nogales, E. Refined structure of $\alpha\beta$-tubulin at 3.5 Å resolution. *J. Mol. Biol.* **2001**, *313*, 1045–1057.

(26) (a) Arnal, I.; Wade, R. H. How does taxol stabilize microtubules? *Curr Biol.* **1995**, *5*, 900–908. (b) Elie-Caille, C.; Severin, F.; Helenius, J.; Howard, J.; Muller, D. J.; Hyman, A. A. Straight GDP-tubulin protofilaments form in the presence of taxol. *Curr. Biol.* **2007**, *17*, 1765–1770.

(27) (a) Krebs, A.; Goldie, K. N.; Hoenger, A. Structural rearrangements in tubulin following microtubule formation. *EMBO Rep.* **2005**, *6*, 227–232. (b) Li, H. L.; DeRosier, D. J.; Nicholson, W. V.; Nogales, E.; Downing, K. H. Microtubule structure at 8 angstrom Resolution. *Structure* **2002**, *10*, 1317–1328.

(28) VanBuren, V.; Odde, D. J.; Cassimeris, L. Estimates of lateral and longitudinal bond energies within the microtubule lattice. *Proc. Natl. Acad. Sci. U.S.A.* **2002**, *99*, 6035–6040.

(29) Verdier-Pinard, P.; Wang, F.; Martello, L.; Burd, B.; Orr, G. A.; Horwitz, S. B. Analysis of tubulin isotypes and mutations from taxol-resistant cells by combined isoelectrofocusing and mass spectrometry. *Biochemistry* **2003**, *42*, 5349–5357.

(30) Martello, L. A.; LaMarche, M. J.; He, L. F.; Beauchamp, T. J.; Smith, A. B., III; Horwitz, S. B. The relationship between Taxol and (+)-discodermolide: Synthetic analogs and modeling studies. *Chem. Biol.* **2001**, *8*, 843–855.

(31) Paterson, I.; Naylor, G. J.; Fujita, T.; Guzman, E.; Wright, A. E. Total synthesis of a library of designed hybrids of the microtubule-stabilising anticancer agents taxol, discodermolide and dictyostatin. *Chem. Commun.* **2010**, *46*, 261–263.

(32) (a) Friesner, R. A.; Banks, J. L.; Murphy, R. B.; Halgren, T. A.; Klicic, J. J.; Mainz, D. T.; Repasky, M. P.; Knoll, E. H.; Shelley, M.; Perry, J. K.; Shaw, D. E.; Francis, P.; Shenkin, P. S. Glide: A new approach for rapid, accurate docking and scoring. 1. Method and assessment of docking accuracy. *J. Med. Chem.* **2004**, *47*, 1739–1749. (b) Halgren, T. A.; Murphy, R. B.; Friesner, R. A.; Beard, H. S.; Frye, L. L.; Pollard, W. T.; Banks, J. L. Glide: A new approach for rapid, accurate docking and scoring. 2. Enrichment factors in database screening. *J. Med. Chem.* **2004**, *47*, 1750–1759.

(33) *Molegro Virtual Docker Software Package*; Molegro ApS: C. F. Moellers Alle 8, Building 1110, DK-8000 Aarhus C, Denmark.

(34) Lyne, P. D.; Lamb, M. L.; Saeh, J. C. Accurate prediction of the relative potencies of members of a series of kinase inhibitors using molecular docking and MM-GBSA scoring. *J. Med. Chem.* **2006**, *49*, 4805–4808.

(35) (a) Barral, K.; Moorhouse, A. D.; Moses, J. E. Efficient conversion of aromatic amines into azides: A one-pot synthesis of triazole linkages. *Org. Lett.* **2007**, *9*, 1809–1811. (b) Xiong, Y.; Bernardi, D.; Bratton, S.; Ward, M. D.; Battaylia, E.; Finel, M.; Drake, R. R.; Radominska-Pandya, A. Phenylalanine 90 and 93 are localized within the phenol binding site of human UDP-glucuronosyltransferase 1A10 as determined by photoaffinity labeling, mass spectrometry, and site-directed mutagenesis. *Biochemistry* **2006**, *45*, 2322–2332. (c) Bernardi, D.; Ba, L. A.; Kirsch, G. First synthesis of *N*-acylated photoactivatable analogues of glutathione bearing an aryl azide moiety. *Synthesis* **2007**, *1*, 140–144.

(36) (a) Hegyi, G.; Michel, H.; Shabanowitz, J.; Hunt, D. F.; Chatterjie, N.; Healylouie, G.; Elzinga, M. Gln-41 is Intermolecularly Cross-Linked to Lys-113 in F-Actin by *N*-(4-Azidobenzoyl)-Putrescine. *Protein Sci.* **1992**, *1*, 132–144. (b) Nielsen, P. E. Photoaffinity Labeling of Chromatin. *Eur. J. Biochem.* **1982**, *122*, 283–289. (c) Borda, E. J.; Sigurdsson, S. T. Investigation of Mg^{2+}- and temperature-dependent folding of the hairpin ribozyme by photo-crosslinking: effects of photo-crosslinker tether length and chemistry. *Nucleic Acids Res.* **2005**, *33*, 1058–1068.

(37) (a) Smith, D. P.; Anderson, J.; Plante, J.; Ashcroft, A. E.; Radford, S. E.; Wilson, A. J.; Parker, M. J. Trifluoromethyldiazirine: an effective photo-induced cross-linking probe for exploring amyloid formation. *Chem. Commun.* **2008**, *11*, 5728–5730. (b) Sammelson, R. E.; Casida, J. E. Synthesis of a tritium-labeled, fipronil-based, highly potent, photoaffinity probe for the GABA receptor. *J. Org. Chem.* **2003**, *68*, 8075–8079. (c) Ambroise, Y.; Pillon, F.; Mioskowski, C.; Valleix, A.; Rousseau, B. Synthesis and tritium labeling of new aromatic diazirine building blocks for photoaffinity labeling and cross-linking. *Eur. J. Org. Chem.* **2001**, *20*, 3961–3964. (d) Krapcho, A. P.; Kuell, C. S. Mono-Protected Diamines *N*-tert-Butoxycarbonyl-alpha,omega-Alkanediamines from alpha,omega-Alkanediamines. *Synth. Commun.* **1990**, *20*, 2559–2564.

(38) Anderson, G. W.; Callahan, F. M.; Zimmerman, J. E. Use of Esters of *N*-Hydroxysuccinimide in Peptide Synthesis. *J. Am. Chem. Soc.* **1964**, *86*, 1839–1844.

(39) Paul, R.; Anderson, G. W. *N*,*N*′-Carbonyldiimidazole, a new peptide forming reagent. *J. Am. Chem. Soc.* **1960**, *82*, 4596–4600.

(40) Anderson, G. W.; Mcgregor, A. C. *tert*-Butyloxycarbonylamino Acids and their use in Peptide Synthesis. *J. Am. Chem. Soc.* **1957**, *79*, 6180–6183.

(41) Kavallaris, M. Microtubules and resistance to tubulin-binding agents. *Nature Rev. Cancer* **2010**, *10*, 194–204.